FULL PAPER

Dalton
www.rsc.org/dalton

Monomeric, trimeric and polymeric assemblies of dicopper(II) complexes of a triazolate-containing Schiff-base macrocycle †

Craig V. Depree, Udo Beckmann, Katie Heslop and Sally Brooker *
Department of Chemistry, University of Otago, PO Box 56, Dunedin, New Zealand.
E-mail: sbrooker@alkali.otago.ac.nz

Received 28th April 2003, Accepted 4th June 2003
First published as an Advance Article on the web 2nd July 2003

The new triazolate-containing Schiff-base macrocyclic ligand $L2^{2-}$ has been synthesised as $[Pb^{II}_2(L2)](ClO_4)_2$, **1**, by the [2 + 2] cyclisation reaction of 3,5-diacetyl-1*H*-1,2,4-triazole and 1,3-diaminopropane using lead(II) template ions. The macrocycle provides four nitrogen atoms, two imine and two triazolate donors, as equatorial donor atoms to each of the two metal ions in the macrocycle. A series of copper(II) complexes of the $L2^{2-}$ macrocycle has been produced with a variety of axial donors. Each copper complex has been structurally characterised by X-ray diffraction and three different structural types can be distinguished: monomeric, trimeric and polymeric. These different types arise from adding a different ratio of thiocyanate ions to the copper(II) transmetallation reaction of $[Pb^{II}_2(L2)](ClO_4)_2$ (**1**). The monomeric dicopper(II) macrocyclic complexes include $[Cu^{II}_2(L2)(NCMe)_2](ClO_4)_2$ (**2**) and $[Cu^{II}_2(L2)(NCS)_2]$ (**3**). The trimeric complex $\{[Cu^{II}_2(L2)]_3(NCS)_2\}(ClO_4)_4$ (**4**) consists of three dicopper(II) macrocyclic complexes bridged by two thiocyanate ions. The thiocyanate-bridged polymeric complex $\{[Cu^{II}_2(L2)(NCS)][Cu^{II}_2(L2)(SCN)](ClO_4)_2\}_x$ (**5**) comprises two types of macrocyclic units in the repeating unit. A second polymeric isomer $\{[Cu^{II}_2(L2)(NCS)](ClO_4)\}_x$ (**6**), incorporating a more symmetrical thiocyanate-bridging mode that has only one type of macrocyclic unit in the repeating unit, is also reported.

Introduction

The Schiff-base macrocycle obtained from the [2 + 2] condensation of 3,6-diformylpyridazine[1,2] and 1,3-diaminopropane, L1 (Fig. 1), has facilitated the isolation of a wide range of transition metal complexes with interesting redox and magnetic properties.[2–5] Given the considerable current interest in utilising substituted 1,2,4-triazoles as ligands for transition metal ions[6–8] in applications such as new magnetic materials,[7,9–12] and photochemically driven molecular devices,[13] we have incorporated this moiety into Schiff-base macrocycles which are related to L1 (*e.g.* $L2^{2-}$ Fig. 1). Recently, we reported the first structurally characterised complexes of a triazolate-containing macrocycle,[14] specifically some dicobalt(II) complexes of the [2 + 2] Schiff-base macrocycle derived from 3,5-diacetyl-1*H*-1,2,4-triazole[15] and 1,4-diaminobutane. Prior to this, Torres and coworkers have successfully isolated some related triazolate-containing macrocyclic complexes, although none have been structurally characterised to date.[15,16] Alcalde *et al*. have structurally characterised some triazolate-containing macrocycles,[17] however no metal complexes of these macrocycles have been reported. There are many examples of acyclic complexes with bridging triazole or triazolate functionalities in the literature.[6] With respect to dicopper(II) complexes in which the metal centers are bridged by two triazole or triazolate units, only eight complexes, of the acyclic ligands L3, $L4^-$, $L5^-$ and $L6^-$ (Fig. 2), have been structurally characterised to date (see later).[9,11,18–21]

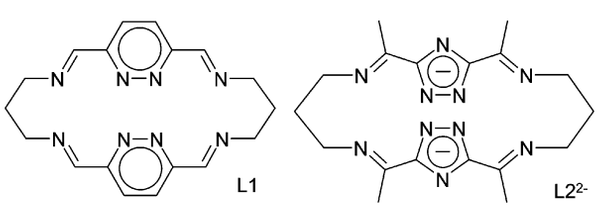

Fig. 1 Ligands L1 and $L2^{2-}$.

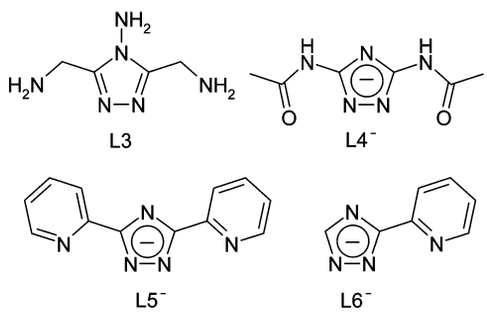

Fig. 2 Ligands L3–$L6^-$.

We report here on the formation and characterisation of the parent lead templated complex $[Pb^{II}_2(L2)](ClO_4)_2$ **1** and six intriguing copper(II) complexes of this new Schiff-base macrocycle, $L2^{2-}$ (Fig. 1); the monomeric acetonitrile adduct $[Cu^{II}_2(L2)(NCMe)_2](ClO_4)_2$ **2**, the monomeric thiocyanate adduct $[Cu^{II}_2(L2)(NCS)_2]$ **3**, a thiocyanate bridged trimer $\{[Cu^{II}_2(L2)]_3(NCS)_2\}(ClO_4)_4$ **4**, and two thiocyanate bridged polymeric structures; $\{[Cu^{II}_2(L2)(NCS)][Cu^{II}_2(L2)(SCN)](ClO_4)_2\}_x$ **5**, and $\{[Cu^{II}_2(L2)(NCS)](ClO_4)\}_x$ **6** (Scheme 1). The different structural motifs are assembled according to the addition of different ratios of thiocyanate ions, increasing in the order from **2**, **4**, **5**, **6**, **3**. These are the first examples of structurally characterised triazolate-containing macrocyclic copper complexes, and as such they represent a significant step forward in the development of the coordination chemistry of this, and related, ligand systems.[14,22]

Results and discussion

Synthesis and characterisation

The $L2^{2-}$ Schiff-base macrocycle is formed by the addition of $Pb(ClO_4)_2 \cdot 6H_2O$ to a solution of 3,5-diacetyl-1*H*-1,2,4-triazole and NaOH in methanol, followed by heating to reflux and the dropwise addition of a methanolic solution of 1,3-diaminopropane. The resulting precipitate was extracted with acetonitrile (the infrared spectrum of the small amount of residual yellowish solid indicated that it was not cyclic in nature) to give,

† Electronic supplementary information (ESI) available: Geometric data for complexes **1**–**6**. See http://www.rsc.org/suppdata/dt/b3/b304658c/

DOI: 10.1039/b304658c

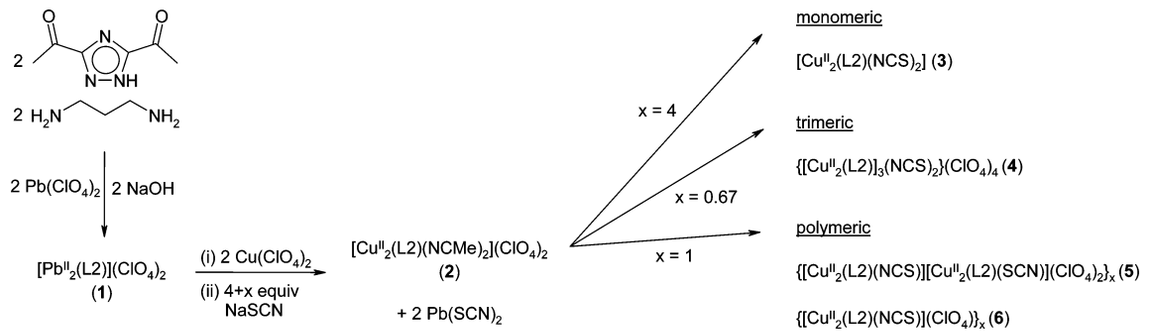

Scheme 1

after evaporation of the acetonitrile solution, the pure lead(II) complex $[Pb^{II}_2(L2)](ClO_4)_2$ **1** in 80% yield. The band at 1635 cm^{-1} in the IR spectrum shows that an imine bond has formed, and the band at 1095 cm^{-1} clearly indicates the presence of perchlorate anions. Colourless crystals suitable for X-ray analysis were obtained *via* slow vapour diffusion of *tert*-butyl methyl ether into an acetonitrile solution of **1**.

Copper(II) complexes of $L2^{2-}$ were prepared by transmetallation of **1** in MeCN with two equivalents of $Cu(ClO_4)_2 \cdot 6H_2O$. Normally the resulting transmetallation solution would simply have been concentrated, resulting in either the precipitation of the desired complex or in a solution which on vapour diffusion of diethyl ether would yield the desired complex. In this case, however, vapour diffusion of diethyl ether into the concentrated dark green transmetallation reaction solution caused the colour to fade and a white, presumably lead-containing, precipitate to form. It was therefore found to be necessary to remove the lead(II) ions from the transmetallation reaction solution before the isolation of the transition metal complex. This was achieved by the addition of a stoichiometric amount (4 equiv. per macrocycle) of thiocyanate ions to the reaction solution, on completion of the transmetallation process, to precipitate the displaced Pb^{2+} ions as $Pb(SCN)_2$.

The copper complex, $[Cu^{II}_2(L2)(NCMe)_2](ClO_4)_2$ (**2**), was readily crystallised from the filtered, Pb^{2+}-free, dark green reaction solution by diethyl ether diffusion. The band of the imine bond shifts to 1621 cm^{-1} and shows that the macrocycle is still intact. The strong band at 1089 cm^{-1} indicates the presence of perchlorate anions. No SCN^- band is present. Green crystals suitable for X-ray analysis were grown in 66% yield by slow diffusion of diethyl ether into the acetonitrile solution. Despite our expectation that copper(II) ions should be able to template the formation of the $L2^{2-}$ macrocycle, thus avoiding the relative complexities of the above transmetallation reaction, the few attempts made to date have not been successful. The problem appears to be the insolubility of at least one intermediate in the cyclisation process.

Thiocyanate ions are asymmetric ligands that have coordination capabilities at both termini. This leads to two monodentate binding modes, N-bound and S-bound, and a variety of bridging modes such as >NCS, >SCN, –NCS– and >SCN– .[23] For our system it was found that different copper complexes of $L2^{2-}$ could be isolated depending on the amount of NaSCN added. The resulting monomeric, trimeric and polymeric motifs are discussed next (Scheme 1).

The monomeric complex $[Cu^{II}_2(L2)(NCS)_2]$ **3** was prepared from the transmetallation solution by using 8.00 equivalents of NaSCN per macrocycle. After filtration to remove the $Pb(SCN)_2$ (consumes 4 equiv. of SCN^-), diethyl ether diffusion into the green acetonitrile solution afforded green crystals in 64% yield, which were suitable for X-ray diffraction. The IR spectrum shows that the macrocycle is still intact, that SCN^- is present (strong band at 2116 cm^{-1}) and that no perchlorate anions are present.

Addition of 4.67 [0.67 equiv. free SCN^- per dicopper(II) macrocycle] equivalents of NaSCN per macrocycle to the acetonitrile transmetallation reaction solution gave the trimer of dicopper(II) macrocyclic complexes, $\{[Cu^{II}_2(L2)]_3(NCS)_2\}(ClO_4)_4$ **4**. Diffusion of diethyl ether into the acetonitrile filtrate gave single crystals of **4** as dark blue wedges in 61% yield. The infrared spectrum of **4** shows that the macrocycle is intact and that SCN^- is present (strong band at 2144 cm^{-1}).

When 5.00 equivalents of NaSCN per macrocycle are added [1 equiv. free SCN^- per dicopper(II) macrocycle], a polymer of dicopper(II) complexes $\{[Cu^{II}_2(L2)(NCS)][Cu^{II}_2(L2)(SCN)](ClO_4)_2\}_x$ **5** is obtained from the transmetallation solution. Blue–green block crystals of $\mathbf{5}\cdot H_2O$ were obtained, in 59% yield, by diffusion of diethyl ether into the acetonitrile filtrate. An imine stretch is observed at 1617 cm^{-1}. In addition, the SCN^- stretch is observed at 2135 cm^{-1} and there is no evidence of amine or carbonyl absorptions. This complex comprises two different macrocyclic structural units in the polymer on account of the organisation of the 1,3-bridging mode of the two thiocyanate ions: both of the copper(II) ions in one macrocyclic unit have N-bound thiocyanate ions whereas in the second macrocyclic unit both copper(II) ions have S-bound thiocyanate ions (see later).

The second polymeric product $\{[Cu^{II}_2(L2)(NCS)](ClO_4)\}_x$ **6** was also obtained by the addition of 5.00 equivalents of NaSCN, but the crystals formed by vapour diffusion of diethyl ether into acetonitrile were redissolved in DMF. Diffusion of diethyl ether into the DMF solution yielded blue–green crystals of **6**·DMF suitable for X-ray analysis. The imine stretch is again observed at 1617 cm^{-1} and the SCN^- stretch at 2130 cm^{-1}. In contrast to **5**, this isomer consists of only one macrocycle structural type in the repeat unit of the polymer on account of the different relative organisation of the 1,3-bridging mode of the two thiocyanate ions resulting in each dicopper(II) macrocyclic unit having one N-bound and one S-bound thiocyanate ion (see later).

The polymeric structural motif observed in **6**·DMF has also been observed in the acetonitrile solvate, **6**·MeCN (see later). It was prepared by redissolving **6**·DMF in acetonitrile and growing crystals by vapour diffusion of diethyl ether. Subsequent X-ray analysis of the crystals showed the structure of **6**·MeCN to be same as **6**·DMF, as opposed to the alternating S-bound and N-bound macrocyclic arrangement observed for $\mathbf{5}\cdot H_2O$.

Reproducing the preparation of the trimer **4** was not straightforward, with the difference in the amount of NaSCN added being only 0.03 mmol (*ca.* 2 mg). Improved accuracy of the reaction stoichiometry, and hence reproducibility of this synthesis, should be possible if significantly larger scale reactions were to be employed. In addition, controlling the selective formation of **5** *vs.* **6** was also found to be difficult, presumably on account of a number of contributing factors, including controlling exactly the ratio of reagents, the solvent and possibly the temperature.[24]

In addition to providing proof of the macrocycle remaining intact, the IR spectra of complexes **3**–**6** also provide us with the ν(CN) stretching frequency of the SCN^- ligands. In these complexes this value is in the range from 2116 to 2144 cm^{-1}. The

Table 1 Selected interatomic distances (Å) and angles (°) for $[Pb^{II}_2(L2)](ClO_4)_2$ (**1**)

Pb(1)–N(1)	2.407(6)	Pb(1) ··· Pb(2)	4.610(2)
Pb(1)–N(4)	2.496(7)	Pb(1)–O(11)	2.825(6)
Pb(1)–N(5)	2.519(7)	Pb(1)–O(12)	3.349(7)
Pb(1)–N(6)	2.430(7)	Pb(1)–O(21)	3.113(8)
Pb(2)–N(2)	2.408(6)	Pb(1A)–O(12)	3.046(7)
Pb(2)–N(7)	2.381(7)	Pb(1A)–O(13)	3.347(7)
Pb(2)–N(9)	2.491(8)	Pb(2)–O(11)	2.844(6)
Pb(2)–N(10)	2.471(7)	Pb(2B)–O(22)	3.348(7)
N(1)–Pb(1)–N(4)	65.3(2)	N(2)–Pb(2)–N(9)	106.7(2)
N(1)–Pb(1)–N(5)	103.3(2)	N(2)–Pb(2)–N(10)	66.3(2)
N(1)–Pb(1)–N(6)	71.9(2)	N(7)–Pb(2)–N(2)	72.4(2)
N(4)–Pb(1)–N(5)	67.5(2)	N(7)–Pb(2)–N(9)	65.9(2)
N(6)–Pb(1)–N(4)	103.5(2)	N(7)–Pb(2)–N(10)	102.8(2)
N(6)–Pb(1)–N(5)	65.0(2)	N(10)–Pb(2)–N(9)	68.0(2)

Symmetry transformations used to generate equivalent atoms: A = 1 − *x*, −*y*, 1 − *z*; B = 1.5 − *x*, −0.5 + *y*, 0.5 − *z*.

Table 2 Selected interatomic distances (Å) and angles (°) for $[Cu^{II}_2(L2)(NCMe)_2](ClO_4)_2$ (**2**)

Cu(1)–N(1)	1.965(2)	Cu(2)–N(7)	1.971(2)
Cu(1)–N(4)	1.998(2)	Cu(2)–N(9)	2.005(2)
Cu(1)–N(5)	2.019(2)	Cu(2)–N(10)	2.005(2)
Cu(1)–N(6)	1.971(2)	Cu(2)–N(40)	2.226(3)
Cu(1)–N(30)	2.188(3)	Cu(1) ··· Cu(2)	4.0664(7)
Cu(2)–N(2)	1.963(2)		
N(1)–Cu(1)–N(6)	92.93(9)	N(2)–Cu(2)–N(7)	91.93(9)
N(1)–Cu(1)–N(4)	80.20(9)	N(2)–Cu(2)–N(9)	153.52(9)
N(6)–Cu(1)–N(4)	152.76(9)	N(7)–Cu(2)–N(9)	80.39(9)
N(1)–Cu(1)–N(5)	153.28(9)	N(2)–Cu(2)–N(10)	80.69(9)
N(6)–Cu(1)–N(5)	80.11(9)	N(7)–Cu(2)–N(10)	152.54(9)
N(4)–Cu(1)–N(5)	94.20(9)	N(9)–Cu(2)–N(10)	94.48(9)
N(1)–Cu(1)–N(30)	101.74(10)	N(2)–Cu(2)–N(40)	102.60(9)
N(6)–Cu(1)–N(30)	107.01(9)	N(7)–Cu(2)–N(40)	104.82(9)
N(4)–Cu(1)–N(30)	100.21(9)	N(9)–Cu(2)–N(40)	103.85(9)
N(5)–Cu(1)–N(30)	104.97(10)	N(10)–Cu(2)–N(40)	102.60(9)

N-bound thiocyanate ions in the monomeric complex **3** give rise to the lowest of these values, 2116 cm^{-1}. As one would anticipate the –NCS– bound thiocyanate ions in **4**–**6** produce values well above 2100 cm^{-1} (2130–2144 cm^{-1}), however, all of these frequencies should be interpreted with caution as they are affected by many other factors.[25]

X-Ray structure determinations

Structure of $[Pb^{II}_2(L2)](ClO_4)_2$ (1). The structure determination of **1**·MeCN reveals a perchlorate-bridged dimer of complex dications, with the macrocycle bonded to the lead atoms in the expected manner (Fig. 3, Table 1); the triazolate 'head' units doubly bridge the two metal ions and along with the imine nitrogen atoms provide an N_4 donor set to each lead ion. The macrocycle in **1** is significantly folded with the triazolate ring planes intersecting at an angle of 69.0(3)°. Both lead atoms are pulled far out of their respective N_4 mean planes [Pb(1) 1.523(3) Å 'out of plane' (oop); Pb(2) 1.485(4) Å oop], which are angled at 35.3(3)° and direct the lead atoms away from each other. The N–Pb–N angles are contracted, reflecting the large displacement of the lead atoms from the N_4 mean planes. The N_{imine}–Pb–$N_{triazolate}$ angles are in the range 65.0–66.3° and the N_{imine}–Pb–N_{imine} and $N_{triazolate}$–Pb–$N_{triazolate}$ angles are in the range 67.5–68.0 and 71.9–72.4°, respectively. There are some weak lead–perchlorate interactions [Pb(1)–O(11) 2.825(6), Pb(1)–O(12) 3.349(7), Pb(1)–O(21) 3.113(8), Pb(1A)–O(12) 3.046(7), Pb(1A)–O(13) 3.347(7), Pb(2)–O(11) 2.844(6), Pb(2B)–O(22) 3.348(7) Å; where A = 1 − *x*, −*y*, 1 − *z* and B = 1.5 − *x*, −0.5 + *y*, 0.5 − *z*], some of which hold the centrosymmetric dimer together.

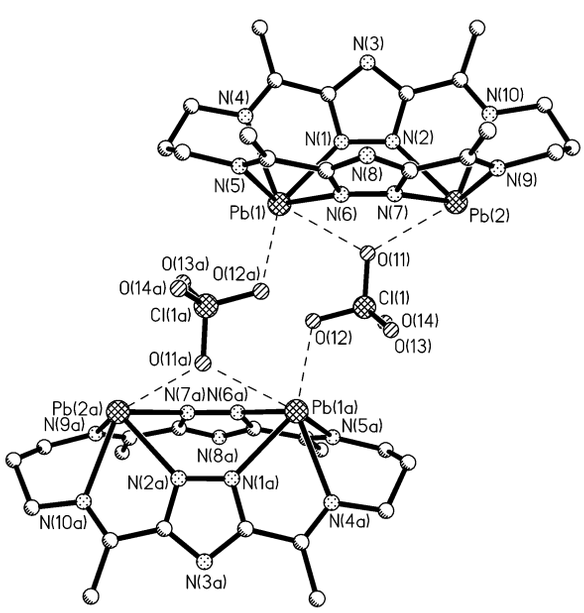

Fig. 3 Perspective view of the cation of **1**, $[Pb^{II}_2(L2)]^{2+}$, which has dimerised *via* a set of interactions with perchlorate counter ions to form $\{[Pb^{II}_2(L2)(ClO_4)]^+\}_2$. Solvent molecules, hydrogen atoms and the remaining perchlorate counter ions have been omitted for clarity.

Structure of $[Cu^{II}_2(L2)(NCMe)_2](ClO_4)_2$ (2). The X-ray structure determination (Fig. 4, Table 2) shows that the transmetallation has occurred and the two lead ions have been replaced by two copper ions. Both copper(II) centers are five coordinate and are bridged by the two triazolate units of the macrocyclic framework. The macrocycle also contributes a further two imine N-donors to each copper center to complete the N_4 equatorial base. The axial position of each Cu(II) center is occupied by a coordinated acetonitrile solvent molecule. The Cu(II) coordination geometry is distorted square pyramidal, similar to the closely related pyridazine-bridged complex[3] $[Cu^{II}_2(L1)(NCMe)_2]^{4+}$. The copper atoms are pulled out of the N_4 basal plane by 0.464(1) and 0.463(1) Å, for Cu(1) and Cu(2), respectively. The N_{imine}–Cu–$N_{triazolate}$ angles are in the range 80.1–80.7° and the N_{imine}–Cu–N_{imine} and $N_{triazolate}$–Cu–$N_{triazolate}$ in the ranges 94.2–94.5 and 91.9–92.9°, respectively. The macrocycle unit is significantly folded with a triazolate ring plane intersection angle of 69.4(1)° and N_4 basal planes angled at 35.17(8)°. The acetonitrile donors have an approximately linear binding angle [C(30)–N(30)–Cu(1) 168.0(3), C(40)–N(40)–Cu(2) 168.9(3)°]. One acetonitrile molecule is also present in the lattice. The copper–copper separation is 4.0664(7) Å.

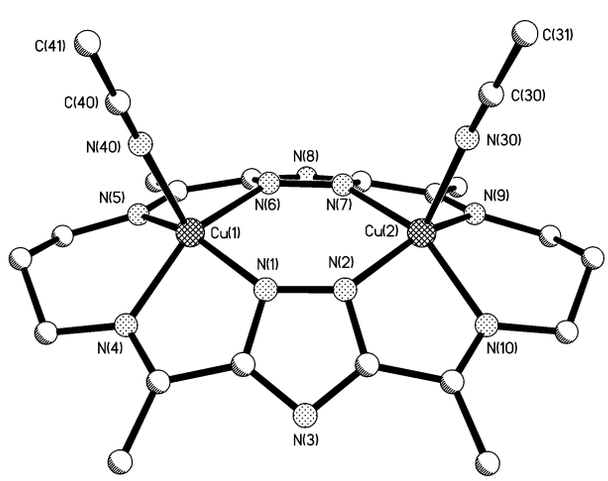

Fig. 4 Perspective view of the cation of **2**, $[Cu^{II}_2(L2)(NCMe)_2]^{2+}$. Solvent molecules, counter ions and hydrogen atoms have been omitted for clarity.

Table 3 Selected interatomic distances (Å) and angles (°) for $[Cu^{II}_2(L2)(NCS)_2]$ (**3**)

Cu(1)–N(1)	1.947(7)	Cu(2)–N(7)	1.964(8)
Cu(1)–N(4)	2.034(7)	Cu(2)–N(9)	2.028(6)
Cu(1)–N(5)	2.003(7)	Cu(2)–N(10)	2.010(7)
Cu(1)–N(6)	1.977(6)	Cu(2)–N(60)	2.107(6)
Cu(1)–N(50)	2.095(7)	Cu(1) ··· Cu(2)	4.075(3)
Cu(2)–N(2)	1.989(6)		
N(1)–Cu(1)–N(6)	92.2(3)	N(2)–Cu(2)–N(7)	92.6(3)
N(1)–Cu(1)–N(4)	80.1(3)	N(2)–Cu(2)–N(9)	149.5(2)
N(6)–Cu(1)–N(4)	152.8(2)	N(7)–Cu(2)–N(9)	80.0(3)
N(1)–Cu(1)–N(5)	151.7(2)	N(2)–Cu(2)–N(10)	79.6(3)
N(6)–Cu(1)–N(5)	80.6(3)	N(7)–Cu(2)–N(10)	154.3(2)
N(4)–Cu(1)–N(5)	93.8(3)	N(9)–Cu(2)–N(10)	94.3(3)
N(1)–Cu(1)–N(50)	111.1(3)	N(2)–Cu(2)–N(60)	112.3(2)
N(6)–Cu(1)–N(50)	108.0(2)	N(7)–Cu(2)–N(60)	109.1(3)
N(4)–Cu(1)–N(50)	99.1(3)	N(9)–Cu(2)–N(60)	98.0(2)
N(5)–Cu(1)–N(50)	97.1(3)	N(10)–Cu(2)–N(60)	96.5(3)

Structure of $[Cu^{II}_2(L2)(NCS)_2]$ (3). The X-ray structure determination shows that the fifth, axial, donor atom of each copper(II) atom in the macrocycle unit is the nitrogen of a thiocyanate ion (Fig. 5, Table 3). The complex is monomeric and there is one solvent molecule of acetonitrile present. The copper atoms have distorted square pyramidal geometry as in **2**, and are pulled out of the N_4 basal planes [Cu(1) 0.477(3), Cu(2) 0.485(3) Å oop]. The N_{imine}–Cu–$N_{triazolate}$ angles are in the range 79.6–80.6°, while N_{imine}–Cu–N_{imine} and $N_{triazolate}$–Cu–$N_{triazolate}$ angles are in the ranges 93.8–94.3 and 92.2 and 92.6°, respectively. There is again a significant fold in the macrocycle with the triazolate planes intersecting at 69.1(2)° and the basal N_4 planes intersecting at 39.8(1)°. The thiocyanate donors are slightly asymmetrically located above the basal planes towards imine donors on opposite corners of the macrocycle unit, as shown by the N–Cu–$N_{thiocyanate}$ angles [N(1)–Cu(1)–N(50) 111.1(3), N(6)–Cu(1)–N(50) 108.0(2), N(5)–Cu(1)–N(50) 97.1(3), N(4)–Cu(1)–N(50) 99.1(3)°] and N(7)–Cu(2)–N(60) 109.1(3), N(2)–Cu(2)–N(60) 112.3(2), N(10)–Cu(2)–N(60) 96.5(3), N(9)–Cu(2)–N(60) 98.0(2)°]. The thiocyanate donors are very slightly bent towards one side of the macrocycle unit [Cu(1)–N(50)–C(50) 161.3(7), Cu(2)–N(60)–C(60) 162.6(6)°]. The copper–copper separation is 4.075(3) Å. There are no significant intermolecular interactions in the crystal lattice.

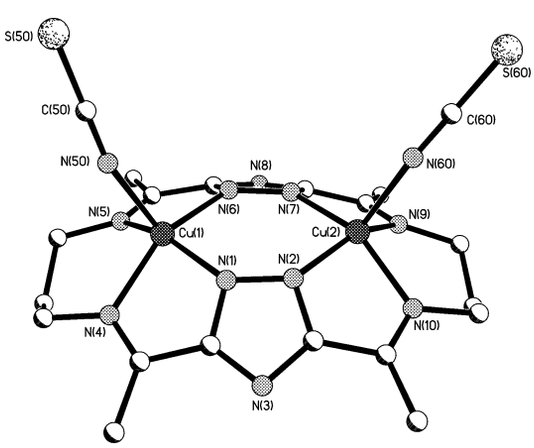

Fig. 5 Perspective view of **3**, $[Cu^{II}_2(L2)(NCS)_2]$. Solvent molecules and hydrogen atoms have been omitted for clarity.

Structure of $\{[Cu^{II}_2(L2)]_3(NCS)_2\}(ClO_4)_4$ (4). The structure determination of **4**·1.5MeCN (Fig. 6, Table 4) shows a trimeric complex cation constructed from three dicopper(II) $L2^{2-}$ macrocycle units and two thiocyanate bridges, in accordance with the reaction stoichiometry [*i.e.* 0.67 equivalents of SCN^- per dicopper(II) macrocycle]. The sulfur donors of the thiocyanate ions each bridge two copper centres from different macrocycles, while the nitrogen donors coordinate to the

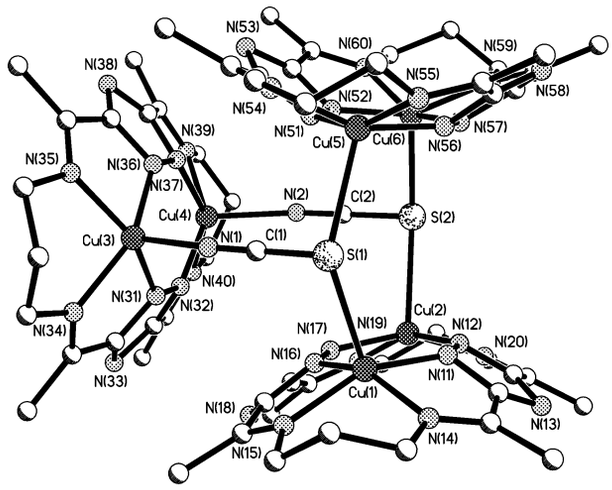

Fig. 6 Perspective view of the cation of **4**, $\{[Cu^{II}_2(L2)]_3(NCS)_2\}^{4+}$. Solvent molecules, counter ions and hydrogen atoms have been omitted for clarity.

copper centres in the single remaining macrocycle unit. The copper atoms have distorted square pyramidal geometries, each with the basal N_4 plane comprised of two N_{imine} and two $N_{triazolate}$ donors. The fifth donor atom for Cu(3) and Cu(4) is the nitrogen atom of a bridging thiocyanate ion, giving an N_5 donor set, while for the remaining four copper atoms it is the sulfur of a bridging thiocyanate ion, giving an N_4S donor set. The N_{imine}–Cu–$N_{triazolate}$ angles are in the range 79.9–80.4° for the copper atoms in the N_5 donor set and are between 80.0–81.0° for the copper atoms in the N_4S donor set and are thus almost identical. Again these angles at copper are significantly less than the ideal value of 90° expected for square pyramidal geometry. The N_{imine}–Cu–N_{imine} and $N_{triazolate}$–Cu–$N_{triazolate}$ angles range from 91.4–95.3 and 92.3–93.3°, respectively. The macrocycles are significantly folded with triazolate plane intersection angles of 70.3(2) and 70.3(3)° for the S-bound macrocycles and 78.3(2)° for the N-bound. The copper atoms are pulled out of the N_4 plane slightly more for the N-bound macrocycle [Cu(3) 0.510(3), Cu(4) 0.523(3) Å oop; N_4 planes intersect at 34.7(2)°] than for the S-bound macrocycle [Cu(1) 0.455(3), Cu(2) 0.435(3) Å oop; N_4 planes intersect at 33.9(2)°; Cu(5) 0.416(3), Cu(6) 0.461(3) Å oop; N_4 planes intersect at 33.1(2)°]. The preference for a near linear binding angle[26] of the thiocyanate through nitrogen [Cu(3)–N(1)–C(1) 171.1(6)°, Cu(4)–N(2)–C(2) 160.0(5)°] and a bent angle for binding through sulfur [Cu(1)–S(1)–C(1) 95.9(2), Cu(2)–S(2)–C(2) 94.1(2), Cu(5)–S(1)–C(1) 93.8(2), Cu(6)–S(2)–C(2) 96.7(2)°] is met. The Cu–S–Cu bridging angles are 136.11(8)° [Cu(1)–S(1)–Cu(5)] and 138.19(7)° [Cu(2)–S(2)–Cu(6)]. The copper–copper separations in each macrocycle are 4.030(2) [Cu(1), Cu(2)] and 4.027(2) Å [Cu(5), Cu(6)] for the S-bound and 4.061(2) Å [Cu(3), Cu(4)] for the N-bound macrocycle.

There are many examples of structurally characterised thiocyanate-bridged copper complexes in the literature where three copper centers are bridged in a Cu_2>SCN–Cu fashion.[27–29] However, all of these complexes are polymeric copper(I) species, except for a mixed-valent Cu^I thiocyanate-bridged polymer with a $[Cu^{II}(DMF)_4]^{2+}$ counterion[29] and a non-polymeric copper(I)–tungsten adduct.[28] None of these structures contains a thiocyanate ion bridging copper(II) centers. The trimeric complex **4** is therefore the first structurally characterised copper(II) complex with a thiocyanate ion present in a Cu^{II}_2>SCN–Cu^{II} bridging mode.

Structure of $\{[Cu^{II}_2(L2)(NCS)][Cu^{II}_2(L2)(SCN)](ClO_4)_2\}_x$ (5). The X-ray structure determination of **5**·H_2O (Fig. 7, Table 5) reveals a polymeric structure, resulting from the 1,3-bridging by thiocyanate ions. The bridging arrangement of the thiocyanate

Table 4 Selected interatomic distances (Å) and angles (°) for $\{[Cu^{II}_2(L2)]_3(NCS)_2\}(ClO_4)_4$ (**4**)

Cu(1)–N(11)	1.959(5)	Cu(4)–N(39)	2.006(6)
Cu(1)–N(14)	1.999(6)	Cu(4)–N(40)	2.016(6)
Cu(1)–N(15)	2.013(6)	Cu(4)–N(2)	2.080(6)
Cu(1)–N(16)	1.953(5)	Cu(5)–N(51)	1.970(6)
Cu(1)–S(1)	2.569(2)	Cu(5)–N(54)	1.985(7)
Cu(2)–N(12)	1.950(5)	Cu(5)–N(55)	1.998(7)
Cu(2)–N(17)	1.968(5)	Cu(5)–N(56)	1.944(6)
Cu(2)–N(19)	1.995(5)	Cu(5)–S(1)	2.590(2)
Cu(2)–N(20)	1.999(5)	Cu(6)–N(52)	1.952(5)
Cu(2)–S(2)	2.6298(19)	Cu(6)–N(57)	1.949(5)
Cu(3)–N(31)	1.970(6)	Cu(6)–N(59)	1.997(5)
Cu(3)–N(34)	2.013(6)	Cu(6)–N(60)	2.001(6)
Cu(3)–N(35)	2.005(6)	Cu(6)–S(2)	2.5144(19)
Cu(3)–N(36)	1.966(5)	Cu(1) ··· Cu(2)	4.030(2)
Cu(3)–N(1)	2.139(6)	Cu(3) ··· Cu(4)	4.061(2)
Cu(4)–N(32)	1.967(6)	Cu(5) ··· Cu(6)	4.027(2)
Cu(4)–N(37)	1.969(6)		
N(11)–Cu(1)–N(14)	80.8(2)	N(32)–Cu(4)–N(37)	92.3(2)
N(11)–Cu(1)–N(15)	153.4(2)	N(32)–Cu(4)–N(39)	148.5(2)
N(14)–Cu(1)–N(15)	93.8(2)	N(32)–Cu(4)–N(40)	80.2(2)
N(16)–Cu(1)–N(11)	93.2(2)	N(37)–Cu(4)–N(39)	79.9(2)
N(16)–Cu(1)–N(14)	153.4(2)	N(37)–Cu(4)–N(40)	150.5(2)
N(16)–Cu(1)–N(15)	80.0(2)	N(39)–Cu(4)–N(40)	91.6(3)
N(11)–Cu(1)–S(1)	109.38(17)	N(32)–Cu(4)–N(2)	106.0(2)
N(14)–Cu(1)–S(1)	106.30(18)	N(37)–Cu(4)–N(2)	103.5(2)
N(15)–Cu(1)–S(1)	97.15(18)	N(39)–Cu(4)–N(2)	105.4(2)
N(16)–Cu(1)–S(1)	100.15(17)	N(40)–Cu(4)–N(2)	106.0(2)
N(12)–Cu(2)–N(17)	92.8(2)	N(51)–Cu(5)–N(54)	81.0(3)
N(12)–Cu(2)–N(19)	154.9(2)	N(51)–Cu(5)–N(55)	155.3(3)
N(12)–Cu(2)–N(20)	80.9(2)	N(54)–Cu(5)–N(55)	95.3(3)
N(17)–Cu(2)–N(19)	80.2(2)	N(56)–Cu(5)–N(51)	93.3(2)
N(17)–Cu(2)–N(20)	154.2(2)	N(56)–Cu(5)–N(54)	156.0(3)
N(19)–Cu(2)–N(20)	94.9(2)	N(56)–Cu(5)–N(55)	80.1(3)
N(12)–Cu(2)–S(2)	102.89(16)	N(51)–Cu(5)–S(1)	101.56(16)
N(17)–Cu(2)–S(2)	107.50(16)	N(54)–Cu(5)–S(1)	95.79(18)
N(19)–Cu(2)–S(2)	102.17(15)	N(55)–Cu(5)–S(1)	103.1(2)
N(20)–Cu(2)–S(2)	98.29(15)	N(56)–Cu(5)–S(1)	108.24(18)
N(31)–Cu(3)–N(34)	80.2(3)	N(52)–Cu(6)–N(59)	154.0(2)
N(31)–Cu(3)–N(35)	150.6(2)	N(52)–Cu(6)–N(60)	80.5(2)
N(35)–Cu(3)–N(34)	91.4(3)	N(57)–Cu(6)–N(52)	92.6(2)
N(36)–Cu(3)–N(31)	92.8(2)	N(57)–Cu(6)–N(59)	80.5(2)
N(36)–Cu(3)–N(34)	150.0(2)	N(57)–Cu(6)–N(60)	152.1(2)
N(36)–Cu(3)–N(35)	80.4(2)	N(59)–Cu(6)–N(60)	93.9(2)
N(31)–Cu(3)–N(1)	106.0(2)	N(52)–Cu(6)–S(2)	105.37(16)
N(34)–Cu(3)–N(1)	102.2(2)	N(57)–Cu(6)–S(2)	106.74(17)
N(35)–Cu(3)–N(1)	103.4(3)	N(59)–Cu(6)–S(2)	100.67(17)
N(36)–Cu(3)–N(1)	107.8(2)	N(60)–Cu(6)–S(2)	101.18(17)

Symmetry transformations used to generate equivalent atoms: A = $-x$, $-y + 2$, $-z + 1$.

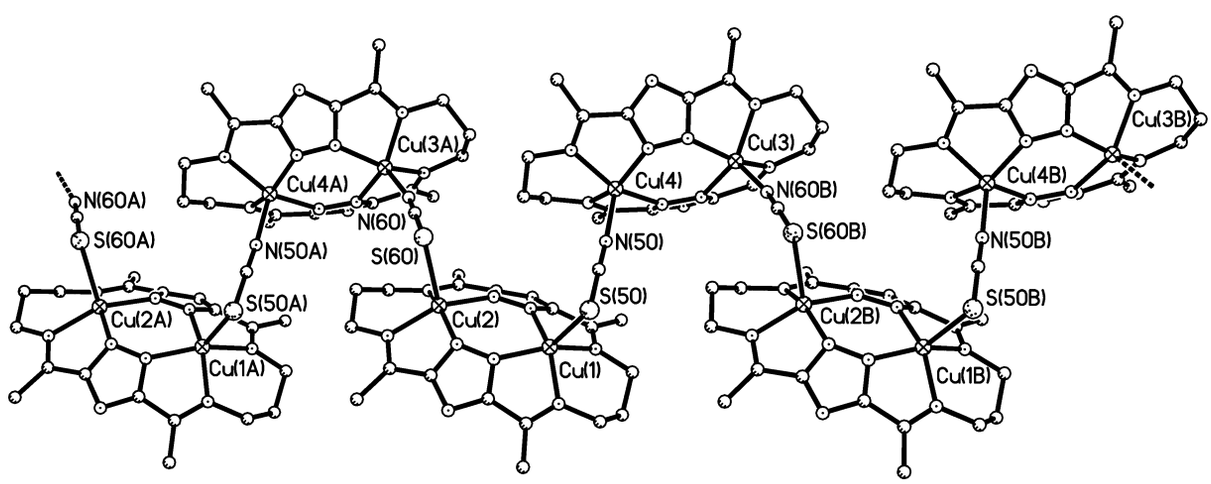

Fig. 7 Perspective view of the cation of **5**, $\{[Cu^{II}_2(L2)(NCS)][Cu^{II}_2(L2)(SCN)]^{2+}\}_x$. Solvent molecules, counter ions and hydrogen atoms have been omitted for clarity.

ligands has resulted in two distinct types of dicopper(II) triazolate macrocycles in the polymer repeating unit. In the first type of complex [Cu(1) and Cu(2)] the fifth donor atoms are the sulfur atoms of the 1,3-bridging thiocyanate ions (S-bound form) whereas in the second type of complex [Cu(3) and Cu(4)] the fifth donor atoms are the nitrogens of these thiocyanate ions (N-bound form). The $L2^{2-}$ macrocycle provides two N_{imine} and two $N_{triazolate}$ donors to the basal plane of each copper atom

Table 5 Selected interatomic distances (Å) and angles (°) for $\{[Cu^{II}_2(L2)(NCS)][Cu^{II}_2(L2)(SCN)](ClO_4)_2\}_x$ (**5**)

Cu(1)–N(1)	1.957(3)	Cu(3)–N(15)	2.023(3)
Cu(1)–N(6)	1.962(3)	Cu(3)–N(60B)	2.089(3)
Cu(1)–N(4)	1.998(3)	Cu(4)–N(17)	1.977(3)
Cu(1)–N(5)	2.010(3)	Cu(4)–N(12)	1.982(3)
Cu(1)–S(50)	2.5073(10)	Cu(4)–N(20)	2.012(3)
Cu(2)–N(7)	1.947(3)	Cu(4)–N(19)	2.018(3)
Cu(2)–N(2)	1.967(3)	Cu(4)–N(50)	2.079(3)
Cu(2)–N(10)	1.986(3)	Cu(1) ··· Cu(2)	4.050(1)
Cu(2)–N(9)	2.002(3)	Cu(3) ··· Cu(4)	4.081(1)
Cu(2)–S(60)	2.5945(11)	Cu(1) ··· Cu(4)	5.737(1)
Cu(3)–N(11)	1.971(3)	Cu(2) ··· Cu(4)	7.020(2)
Cu(3)–N(16)	1.983(3)	Cu(1) ··· Cu(3)	8.720(2)
Cu(3)–N(14)	2.003(3)	Cu(2) ··· Cu(3)	10.934(3)
N(1)–Cu(1)–N(6)	92.41(11)	N(11)–Cu(3)–N(16)	91.50(11)
N(1)–Cu(1)–N(4)	80.93(11)	N(11)–Cu(3)–N(14)	80.13(11)
N(6)–Cu(1)–N(4)	153.57(11)	N(16)–Cu(3)–N(14)	146.40(11)
N(1)–Cu(1)–N(5)	154.66(11)	N(11)–Cu(3)–N(15)	150.78(11)
N(6)–Cu(1)–N(5)	80.16(11)	N(16)–Cu(3)–N(15)	79.73(12)
N(4)–Cu(1)–N(5)	94.96(11)	N(14)–Cu(3)–N(15)	91.83(12)
N(1)–Cu(1)–S(50)	109.97(8)	N(11)–Cu(3)–N(60B)	102.85(11)
N(6)–Cu(1)–S(50)	109.69(8)	N(16)–Cu(3)–N(60B)	112.43(11)
N(4)–Cu(1)–S(50)	96.58(8)	N(14)–Cu(3)–N(60B)	101.17(12)
N(5)–Cu(1)–S(50)	95.32(8)	N(15)–Cu(3)–N(60B)	106.27(12)
N(7)–Cu(2)–N(2)	92.16(11)	N(17)–Cu(4)–N(12)	91.84(11)
N(7)–Cu(2)–N(10)	156.10(11)	N(17)–Cu(4)–N(20)	152.40(11)
N(2)–Cu(2)–N(10)	81.32(11)	N(12)–Cu(4)–N(20)	80.25(11)
N(7)–Cu(2)–N(9)	80.75(11)	N(17)–Cu(4)–N(19)	79.84(12)
N(2)–Cu(2)–N(9)	152.74(11)	N(12)–Cu(4)–N(19)	147.18(11)
N(10)–Cu(2)–N(9)	94.54(11)	N(20)–Cu(4)–N(19)	92.54(12)
N(7)–Cu(2)–S(60)	101.21(8)	N(17)–Cu(4)–N(50)	101.53(11)
N(2)–Cu(2)–S(60)	106.90(8)	N(12)–Cu(4)–N(50)	111.04(11)
N(10)–Cu(2)–S(60)	102.69(8)	N(20)–Cu(4)–N(50)	105.99(12)
N(9)–Cu(2)–S(60)	100.31(8)	N(19)–Cu(4)–N(50)	101.74(12)

Symmetry transformations used to generate equivalent atoms: A = $x - 1$, y, z; B = $x + 1$, y, z.

as before. The copper centres have distorted square pyramidal geometry; N_{imine}–Cu–$N_{triazolate}$ angles range from 79.7–80.1° for the N-bound complex to 80.2–81.3° for the S-bound complex, whereas the N_{imine}–Cu–N_{imine} and $N_{triazolate}$–Cu–$N_{triazolate}$ angles are between 91.5–92.5 and 92.2–95.0°, respectively. The macrocycles are significantly folded, with the triazolate ring planes intersecting at angles of 67.9(1) and 78.3(1)°, for the S-bound and N-bound macrocycles, respectively. As in **4** there is greater folding of the N-bound macrocycle compared to the S-bound macrocycle, and the Cu–N–C angle is approximately linear whereas the Cu–S–C angle is bent [Cu(3)–N(60B)–C(60B) 166.5(3), Cu(4)–N(50)–C(50) 175.3(3), Cu(1)–S(50)–C(50) 95.5(1), Cu(2)–S(60)–C(60) 95.6(1)°]. The S-bound copper atoms are not pulled as far out of the basal N_4 plane [Cu(1) 0.443(1), Cu(2) 0.437(1) Å oop; N_4 planes intersect at 36.2(1)°] as the N-bound copper atoms are [Cu(3) 0.540(1), Cu(4) 0.520(1) Å oop; N_4 planes intersect at 35.4(1)°]. Within the macrocycles the respective copper–copper separations are 4.050(1) [Cu(1), Cu(2)] for the S-bound macrocycle and 4.081(1) Å [Cu(3), Cu(4)] for the N-bound. The polymer chains are arranged in double layers with the thiocyanate 'faces' towards each other and then the alkyl 'faces' of each double layer facing, separated by a channel of perchlorate and water molecules. The chains are staggered within double layers and between double layers.

Structure of $\{[Cu^{II}_2(L2)(NCS)](ClO_4)\}_x$·DMF (6·DMF). In contrast to **5**, the structure of **6** is an alternative polymeric isomer arising from a different combination of the 1,3-bridging modes of the two thiocyanate ions (Fig. 8, Table 6). As opposed to the alternating S-bound and N-bound macrocyclic units of **5**, **6** consists of only one type of macrocycle, with one N-bound and one S-bound thiocyanate ion, in the polymer repeat unit. The polymer chains are arranged in layers with adjacent chains separated by a channel of perchlorate counterions and DMF solvent molecules. Successive layers are staggered. The thiocyanate ions are all in the same direction along the chain, in contrast to **5**, where the bridging thiocyanate ions alternate in orientation. This results in each macrocycle unit having one copper atom with an S-bound thiocyanate as the fifth donor atom, giving an N_4S donor set and the other an N-bound thiocyanate, giving an N_5 donor set. Both copper atoms have distorted square pyramidal geometry and are pulled out of the N_4 basal plane towards the axial thiocyanate donor by 0.433(1) and 0.495(1) Å oop for the N_4S and N_5 donor sets, respectively. The N_{imine}–Cu–$N_{triazolate}$ angles are in the range 79.6–80.2° and the N_{imine}–Cu–N_{imine} and $N_{triazolate}$–Cu–$N_{triazolate}$ angles in the ranges 93.6–96.2 and 92.8–93.1°, respectively. The binding preferences of thiocyanate nitrogen and sulfur donors are again observed with linear coordination to N and bent coordination to S [C(50)–N(50)–Cu(2) 168.7(3), C(50)–S(50)–Cu(1B) 114.38(12)°].

Due to the different orientation of the thiocyanate ions in **5** and **6**, the geometry of the polymer chains is different. In **5**, the unit with two sulfur donors is bent away from the nitrogen bound unit because of the preference of sulfur for a bent angle. In **6**, each unit has one sulfur donor and one nitrogen donor, resulting in a zigzag chain. If the polymers are considered to be in a square tube, in **5** the macrocycle units occupy adjacent sides, whereas in **6** they occupy opposite sides. The fold in the macrocycle in **6** is similar to that in the previous complexes with triazolate ring planes intersecting at 68.2(1)° and N_4 basal planes intersecting at 33.85(8)°. The copper–copper separation is 4.043(1) Å, closer to the values observed for S-bound macrocycles in **4** and **5** than the N-bound macrocycles. There is a weak copper–perchlorate interaction [Cu(1)–O(11) 3.053(3)Å].

Structure of $\{[Cu^{II}_2(L2)(NCS)](ClO_4)\}_x$·MeCN (6·MeCN). The polymer chain is constructed in the same manner as that in **6**·DMF, with bridging thiocyanate ions alternating between nitrogen and sulfur donors (Table 7). The polymer chains are arranged in layers with chains separated by perchlorate counter-

Table 6 Selected interatomic distances (Å) and angles (°) for $\{[Cu^{II}_2(L2)(NCS)](ClO_4)\}_x$·DMF (**6**·DMF)

Cu(1)–N(1)	1.964(3)	Cu(2)–N(7)	1.956(3)
Cu(1)–N(4)	2.020(3)	Cu(2)–N(9)	2.032(3)
Cu(1)–N(5)	1.995(3)	Cu(2)–N(10)	2.022(3)
Cu(1)–N(6)	1.967(3)	Cu(2)–N(50)	2.100(3)
Cu(1)–S(50A)	2.5595(11)	Cu(1) ··· Cu(2)	4.043(1)
Cu(2)–N(2)	1.980(3)		
N(1)–Cu(1)–N(6)	93.07(11)	N(7)–Cu(2)–N(2)	92.77(11)
N(1)–Cu(1)–N(5)	155.57(11)	N(7)–Cu(2)–N(10)	152.89(11)
N(6)–Cu(1)–N(5)	80.16(11)	N(2)–Cu(2)–N(10)	79.80(11)
N(1)–Cu(1)–N(4)	79.62(11)	N(7)–Cu(2)–N(9)	79.73(11)
N(6)–Cu(1)–N(4)	153.93(11)	N(2)–Cu(2)–N(9)	149.72(11)
N(5)–Cu(1)–N(4)	96.17(11)	N(10)–Cu(2)–N(9)	93.56(11)
N(1)–Cu(1)–S(50A)	92.86(8)	N(7)–Cu(2)–N(50)	103.57(12)
N(6)–Cu(1)–S(50A)	103.30(8)	N(2)–Cu(2)–N(50)	108.12(11)
N(5)–Cu(1)–S(50A)	111.52(8)	N(10)–Cu(2)–N(50)	103.52(12)
N(4)–Cu(1)–S(50A)	102.03(8)	N(9)–Cu(2)–N(50)	102.16(11)

Symmetry transformations used to generate equivalent atoms: A = $-x + 1$, $y - ½$, $-z + ½$; B = $-x + 1$, $y + ½$, $-z + ½$.

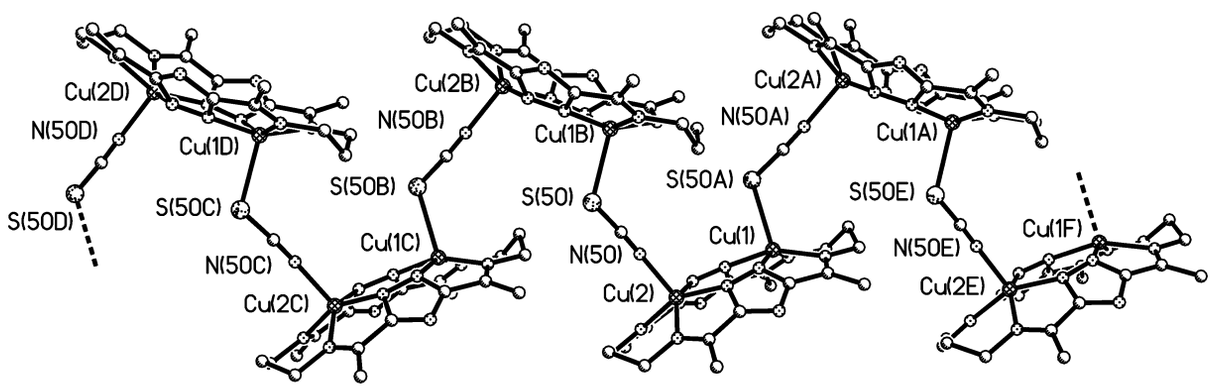

Fig. 8 Perspective view of the cation of **6**, $\{[Cu^{II}_2(L2)(NCS)]^+\}_x$. Solvent molecules, counter ions and hydrogen atoms have been omitted for clarity.

Table 7 Selected interatomic distances (Å) and angles (°) for $\{[Cu^{II}_2(L2)(NCS)](ClO_4)\}_x$·MeCN (**6**·MeCN)

Cu(1)–N(1)	1.972(5)	Cu(2)–N(7)	1.969(5)
Cu(1)–N(4)	2.040(5)	Cu(2)–N(9)	2.025(5)
Cu(1)–N(5)	2.043(5)	Cu(2)–N(10)	2.002(6)
Cu(1)–N(6)	1.970(5)	Cu(2)–S(50)	2.607(2)
Cu(1)–N(50A)	2.104(6)	Cu(1) ··· Cu(2)	4.053(2)
Cu(2)–N(2)	1.971(5)		
N(1)–Cu(1)–N(6)	93.1(2)	N(7)–Cu(2)–N(2)	92.6(2)
N(1)–Cu(1)–N(5)	153.0(2)	N(7)–Cu(2)–N(10)	155.8(2)
N(6)–Cu(1)–N(5)	79.6(2)	N(2)–Cu(2)–N(10)	80.7(2)
N(1)–Cu(1)–N(4)	79.7(2)	N(7)–Cu(2)–N(9)	80.2(2)
N(6)–Cu(1)–N(4)	150.4(2)	N(2)–Cu(2)–N(9)	155.9(2)
N(5)–Cu(1)–N(4)	93.8(2)	N(10)–Cu(2)–N(9)	96.4(2)
N(1)–Cu(1)–N(50A)	103.7(2)	N(7)–Cu(2)–S(50)	91.13(15)
N(6)–Cu(1)–N(50A)	107.1(2)	N(2)–Cu(2)–S(50)	102.70(15)
N(5)–Cu(1)–N(50A)	103.3(2)	N(10)–Cu(2)–S(50)	113.04(15)
N(4)–Cu(1)–N(50A)	102.6(2)	N(9)–Cu(2)–S(50)	100.43(15)

Symmetry transformations used to generate equivalent atoms: A = $-x$, $y + ½$, $-z + ½$; B = $-x$, $y - ½$, $-z + ½$.

ions and acetonitrile solvent molecules. Further layers are staggered slightly and the overall packing of the polymer chains is the same as in the previous structure. The displacement of the copper atoms from the basal N_4 planes is 0.491(3) Å for the N-bound and 0.416(3) Å for the S-bound. Although these values are statistically different from those in **6**·DMF, they are similar and show the same difference between the N-bound and S-bound parts of the macrocycle. The slight difference in absolute values can be explained by the difference in solvent in the two structures and the changes this makes to the cell parameters. There is a weak copper–perchlorate interaction; Cu(2)–O(11) of 3.111(6) Å as seen in **6**·DMF. The copper–copper separation is effectively the same as in **6**·DMF at 4.053(2) Å. The thiocyanate bridges are bound in the expected manner with a near-linear angle at nitrogen and a bent angle at sulfur [C(50)–N(50)–Cu(1B) 174.6(5), C(50)–S(50)–Cu(2) 115.4(2)°]. The fold in the macrocycle results in the triazolate ring planes intersecting at 65.1(2)° and basal N_4 planes intersecting at 34.1(2)°. These values are typical of the structures so far, as are the metal coordination angles: N_{imine}–Cu–$N_{triazolate}$ angles are in the range 79.6–80.7°, while N_{imine}–Cu–N_{imine} and $N_{triazolate}$–Cu–$N_{triazolate}$ angles are in the range 93.8–96.4 and 92.6–93.1°, respectively.

Comparison of the structures. As expected the $L2^{2-}$ macrocycle forms a dicopper(II) complex unit in **2**–**6**. However, the addition of a different ratio of thiocyanate ions after transmetallation results in different supramolecular architectures. All of the structures have copper(II) centres with a distorted square pyramidal geometry. For a given complex, the Cu–N_{imine} bond lengths [range 1.99–2.04 Å; average 2.01 Å] are generally longer than the Cu–$N_{triazolate}$ bond lengths [range 1.94–1.99 Å; average 1.97 Å], (see Table S1, ESI†). This is the reverse trend to that seen in the analogous pyridazine complex[3] $[Cu^{II}_2(L1)(NCMe)_2]^{4+}$ in which the Cu–N_{imine} bond lengths range from 1.96–1.99 Å compared to the Cu–$N_{pyridazine}$ bond lengths with a range of 2.04–2.04 Å. The N_{imine}–Cu–$N_{triazolate}$ angles are smaller than the equivalent pyridazine angles [range 79.6–81.3°; average 80.3°; N_{imine}–Cu–$N_{pyridazine}$ 81.2–81.8°].[3] The N_{imine}–Cu–N_{imine} angles are about the same [range 91.4–96.4°; average 94.0° – compared to 93.3–94.2°] while the $N_{triazolate}$–Cu–$N_{triazolate}$ angles are significantly smaller with range 91.9–95.0°, average 92.6° [$N_{pyridazine}$–Cu–$N_{pyridazine}$ bite angles 99.3–102.1°].[3] These differences can be explained by the presence of a five-membered heterocycle in the $L2^{2-}$ macrocycle compared to a six-membered heterocycle in L1. The effect of this is to angle the N-donors of the imine arms away from the heterocyclic N-donors in $L2^{2-}$ causing, amongst other things, the Cu–N_{imine} bond lengths to be longer. In the L1 macrocycle the imine

N-donors are more in line with the heterocyclic donors which results in somewhat shorter Cu–N_{imine} bonds. Another consequence of the five- *vs.* six-membered ring is a reduction in cavity size. This causes the metal atoms in the triazolate macrocycle to be further displaced from the basal N_4 plane than in the pyridazine macrocycle, and explains the observed contraction in angles for the triazolate macrocycles. This angle contraction is also related to the fold in the macrocycle. The triazolate macrocycles are more folded than the pyridazine analogues; triazolate plane intersection angles in complexes **2**–**6** range from 65.1 to 78.3° {*cf.* $[Cu^{II}_2(L1)(NCMe)_2]^{4+}$ 29.7°} and basal N_4 plane intersection angles range from 33.1 to 36.2° {*cf.* $[Cu^{II}_2(L1)(NCMe)_2]^{4+}$ 9.9°}. The position of the imine arms on the five-membered triazole ring causes the N_4 planes to be angled away from each other when the macrocycle is folded. This does not happen to such an extent for the pyridazine macrocycle as the imine arms are attached to a six-membered ring, and the larger cavity size of the pyridazine macrocycle allows for a flatter arrangement. The fact that the N_4 planes are angled away from each other more and the copper atoms are displaced further from the N_4 plane than in the pyridazine complex, should result in greater Cu ··· Cu separations. The separations [range 4.03–4.08 Å; average 4.05 Å] are, as expected, greater than those seen in the related pyridazine complexes {*cf.* $[Cu^{II}_2(L1)(NCMe)_2]^{4+}$ Cu ··· Cu 3.805(3) Å}.[3]

There are differences between the $L2^{2-}$ macrocycle units when bonded to the nitrogen of a thiocyanate ion compared to those bonded to the sulfur of a thiocyanate ion. The copper atoms with an N_5 donor set are pulled further out of the basal N_4 plane [range 0.46–0.54 Å; average 0.50 Å] than those with an N_4S donor set [range 0.42–0.46 Å; average 0.44 Å]. The greater displacement of the $Cu(N_5)$ atoms combined with the angling away of the N_4 planes in the macrocycle unit also results in the Cu ··· Cu separation for a macrocycle unit with two N_5 donor sets being somewhat longer [range 4.06–4.08 Å; average 4.07 Å] than that with two N_4S donor sets [range 4.03–4.05 Å; average 4.04 Å]. In **6** the macrocycle has one N_5 donor set and one N_4S and has an intermediate value [average Cu ··· Cu 4.05 Å], resulting from one long and one short displacement.

These results can be compared with those obtained from the structural studies carried out by Haasnoot, Reedijk and co-workers on the complexes of the acyclic ligands, L3–$L6^-$, shown in Fig. 2. In the two described complexes of L3, the only ligand containing a triazole instead of a triazolate unit, the two copper centers are octahedrally coordinated and the doubly triazole-bridged dicopper(II) moieties are planar by symmetry.[20] The only amide ligand in this series is $L4^-$, and it gives a dicopper(II) complex with two triazolate ligands bridging the metal centers.[18] The amide oxygen atoms, a water molecule and nitrate anion complete the distorted octahedral coordination sphere of each copper ion. The $[Cu^{II}_2(L4)_2]^{2+}$ cation is planar. By using $L5^-$ instead of $L4^-$ the authors get the analogous complex with the same axial ligands, and a complex with the nitrate anions replaced by weakly coordinated triflate anions.[9] The copper centers are again in a distorted octahedral environment and the two triazolate ring mean planes intersect at the slightly larger angle of 13° in the latter case (no coordinates are available for the former complex). With the triazolate ligand $L6^-$, three dicopper(II) complexes have been prepared, two with octahedral coordination spheres[19] and one with two five-coordinated copper centers.[21] These $[Cu^{II}_2(L6)]^{2+}$ cations are again nearly planar with the intersection angle of the two triazolate ring mean planes being in the range of 0° (planar by symmetry) to 6°. It is interesting to note that within the restrictive framework of the $L2^{2-}$ macrocycle the two triazolate units are no longer co-planar as they are, or very nearly are, in these related acyclic complexes. This is expected to lead to a significant decrease in magnetic exchange interactions, as we showed was the case in a series of closely related, folded, dicobalt(II) complexes.[14]

The Cu–$N_{triazole/triazolate}$ distance in these acyclic complexes of L3–$L6^-$ ranges from 1.93 to 2.01 Å (average 1.97 Å) with no significant difference in a Cu–$N_{triazole}$ and a Cu–$N_{triazolate}$ bond length.[9,11,18–21] The Cu–$N_{triazolate}$ bond lengths in the macrocyclic complexes **2**–**6** described here are about the same (1.94–1.99 Å, average 1.97 Å). The copper–copper separations in **2**–**6** do not differ significantly [range 3.85–4.09 Å; average 4.02 Å] from those observed for these acyclic complexes [4.07–4.09 Å (L3), 3.854(6) Å ($L4^-$), 4.085(1) Å ($L5^-$) and 3.97–4.03 Å ($L6^-$)].

The lead(II) macrocyclic complex is different from the copper(II) series. The [2 + 2] macrocycle has formed in the expected manner but, due to the increased ionic radius, the macrocycle cavity is unable to accommodate the lead atoms, which are consequently pulled much further out of the basal N_4 plane of the macrocycle than the copper atoms are in complexes **2**–**6**. The fold in the $L2^{2-}$ macrocycle is consequently far larger than it is in the copper series, as is shown by the larger triazolate intersection angle of 111.0(3)° (*cf.* average for copper complexes 70.8°), while the N_4 mean plane intersection angle at 35.3(3)° is similar (*cf.* average for copper complexes 35.1°) as this value is fixed by the orientation of the imine arms.

Conclusion

These results, along with our previously reported results[14,22] and those of Torres and co-workers[15,16] using related triazolate ligands, show that macrocyclic triazolate-containing ligands are a promising system for generating interesting coordination complexes. These particular complexes form an unusual set of structurally characterised thiocyanate-bridged assemblies in which a macrocyclic dicopper(II) complex is the basic unit. They also highlight the potential importance of stoichiometric control in assembling interesting arrays or polymers which may optimise the intermolecular communication between metal ion centers. These results will therefore be valuable as we work towards controlling both the effectiveness and the extent of intermolecular communication between metal ions to produce magnetically interesting and potentially useful materials. We[14] and others[6,12] have already shown that the triazolate unit itself is capable of mediating magnetic exchange. Our next aim is to explore this, and related, ligand systems further[22] by varying the transition metals, especially targeting cobalt[14,22] and iron,[12,30] the latter being a strong candidate for giving spin-crossover complexes.

Experimental

3,5-Diacetyl-1*H*-1,2,4-triazole was prepared according to the literature preparation.[15] All reagents and solvents were used as received, without further purification, unless otherwise stated. Acetonitrile was refluxed over calcium hydride and distilled prior to use. Measurements were carried out as described previously.[2,5]

Extreme CAUTION! Whilst no problems were encountered in the course of this work, perchlorate mixtures are potentially explosive and should therefore be handled with appropriate care.

Preparation of the lead precursor complex

$[Pb^{II}_2(L2)](ClO_4)_2$ (1), crystals as 1·MeCN. $Pb(ClO_4)_2·6H_2O$ (1.5 g, 3.26 mmol) was added to a stirred solution of 3,5-diacetyl-1*H*-1,2,4-triazole (500 mg, 3.26 mmol) and NaOH (130 mg, 3.26 mmol) in MeOH (*ca.* 100 mL). As the reaction mixture was heated to reflux temperature, a methanolic solution (2–3 mL) of 1,3-diaminopropane (250 mg, 3.37 mmol) was added dropwise causing the reaction mixture to become cloudy within 15 min. The reaction was stirred at reflux temperature overnight (*ca.* 17 h) producing a fine white precipitate. The precipitate was collected by filtration and dried under vacuum. The

solid was added to MeCN (*ca.* 10 mL per 100 mg) and the small amount of insoluble material was separated by centrifugation. Evaporation of the MeCN yielded colourless microcrystals of $[Pb^{II}_2(L2)](ClO_4)_2$ (1.29 g, 80%). Crystals suitable for X-ray analysis were obtained *via* slow vapour diffusion of *tert*-butyl methyl ether into MeCN solutions of $[Pb^{II}_2(L2)](ClO_4)_2$. FAB *m*/*z* (rel. intensity): 154 (100), 289 (22), 307 (38), 794 (7), 811 (4), 831 (4), 895 (16) $[(Pb_2L2)ClO_4]^+$, 1887 (<1) (dimeric). Found: C, 21.46; H, 2.37; N, 13.81; Cl, 6.70. $C_{18}H_{24}N_{10}Pb_2Cl_2O_8$ requires C, 21.76; H, 2.43; N, 14.09; Cl, 7.14%. IR (KBr disk) (ν_{max}/cm^{-1}): 1635, 1413, 1355, 1095, 619.

Preparation of the copper(II) complexes

$[Cu^{II}_2(L2)(NCMe)_2](ClO_4)_2$ (2), crystals as 2·MeCN. To a heated, stirred solution of $[Pb^{II}_2(L2)](ClO_4)_2$ (100 mg, 0.1 mmol) in MeCN (*ca.*20 mL), was added a solution of $Cu(ClO_4)_2·6H_2O$ (74 mg, 0.2 mmol) in MeCN (3 mL), and the clear blue solution was heated at reflux temperature for 3–4 h. To the resulting intense dark-green solution was added NaSCN (32 mg, 0.4 mmol), which produced an instant precipitate of $Pb(SCN)_2$. The reaction mixture was cooled to room temperature and filtered to remove the $Pb(SCN)_2$. Slow vapour diffusion of diethyl ether into the filtrate yielded dark-green crystals of $[Cu^{II}_2(L2)(NCMe)_2](ClO_4)_2$ which were dried under vacuum (50 mg, 69%). FAB *m*/*z* (rel. intensity): 154 (90), 307 (10), 506 (15) $[Cu^{II}_2L2]^{2+}$, 607 (8) $[(Cu^{II}_2L2)ClO_4]^+$. Found C, 28.98; H, 3.67; N, 18.56. $C_{18}H_{28}N_{10}Cu_2Cl_2O_{10}$ requires C, 29.19; H, 3.81; N, 18.92%. IR (KBr disk) (ν_{max}/cm^{-1}): 1621, 1412, 1359, 1089, 620.

$[Cu^{II}_2(L2)(NCS)_2]$ (3), crystals as 3·MeCN. The same procedure was followed as for $[Cu^{II}_2(L2)(NCMe)_2](ClO_4)_2$ (**2**), except 0.8 mmol (65 mg) NaSCN was added to the reaction mixture. Similarly, the reaction mixture was filtered to remove the $Pb(SCN)_2$ and the filtrate diffused with diethyl ether to yield green crystals of $[Cu^{II}_2(L2)(NCS)_2]$·MeCN (40 mg, 64%). FAB *m*/*z* (rel. intensity): 154 (80), 307 (16), 506 (11), 607 (11). Found C, 38.50; H, 3.76; N, 26.93; S, 10.27. $C_{20}H_{24}N_{12}S_2Cu_2$ requires C, 38.52; H, 3.88; N, 26.95; S, 10.28%. IR (KBr disk) (ν_{max}/cm^{-1}): 2116, 1615, 1489, 1412, 1359, 1227, 622.

$\{[Cu^{II}_2(L2)]_3(NCS)_2\}(ClO_4)_4$ (4), crystals as 4·1.5 MeCN. To a heated, stirred solution of $[Pb^{II}_2(L2)](ClO_4)_2$ (100 mg, 0.101 mmol) in MeCN (*ca.*20 mL), was added a solution of $Cu(ClO_4)_2·6H_2O$ (37 mg, 0.101 mmol) in MeCN (3 mL), and the clear blue solution was heated at reflux temperature for 3–4 h. To the resulting intense dark-green solution was added 4.67 mol equivalents (per macrocycle) of NaSCN (38 mg, 0.47 mmol). The reaction mixture was cooled to room temperature and filtered to remove the $Pb(SCN)_2$ and the blue–green filtrate diffused with diethyl ether to yield dark blue crystals of $\{[Cu^{II}_2(L2)]_3(NCS)_2\}(ClO_4)_4·1.5MeCN$ (42 mg, 61%). FAB *m*/*z* (rel. intensity): 154 (100), 307 (11), 506 (14), 607 (9). Found C, 33.24; H, 3.72; N, 21.92; S, 2.88; Cl, 7.24. $C_{56}H_{72}N_{32}O_{16}S_2Cl_4Cu_6$ requires C, 33.03; H, 3.56; N, 22.01; S, 3.15; Cl, 6.96%. IR (KBr disk) (ν_{max}/cm^{-1}): 2144, 1615, 1417, 1359, 1226, 1089, 622.

$\{[Cu^{II}_2(L2)(NCS)][Cu^{II}_2(L2)(SCN)](ClO_4)_2\}_x$ (5), crystals as 5·H_2O. The same procedure as for $[Cu^{II}_2(L2)(NCMe)_2](ClO_4)_2$ (**2**) was followed, except 5.00 equivalents (per macrocycle) of NaSCN (41 mg, 0.5 mmol) was added to the reaction mixture. Similarly, the reaction mixture was filtered to remove the $Pb(SCN)_2$ and the blue–green filtrate diffused with diethyl ether to yield blue–green crystals of $\{[Cu^{II}_2(L2)(NCS)][Cu^{II}_2(L2)(SCN)](ClO_4)_2\}_x·H_2O$ (42 mg, 59%). FAB *m*/*z* (rel. intensity): 154 (98), 307 (11), 506 (10), 607 (12). Found C, 34.72; H, 3.88; N, 23.69; S, 4.51. $C_{38}H_{48}N_{22}O_8S_2Cl_2Cu_4$ requires C, 34.39; H, 3.65; N, 23.23; S, 4.82%. IR (KBr disk) (ν_{max}/cm^{-1}): 2135, 1617, 1490, 1414, 1361, 1227, 1088, 623.

Table 8 X-Ray data for structure determinations on complexes **1**–**6**

	1·MeCN	**2**·MeCN	**3**·MeCN	**4**·1.5MeCN	**5**·H_2O	**6**·DMF	**6**·MeCN
Emp. formula	$C_{20}H_{27}Cl_2N_{11}O_8Pb_2$	$C_{24}H_{33}Cl_2Cu_2N_{13}O_8$	$C_{22}H_{27}Cu_2N_{13}S_2$	$C_{59}H_{76.50}Cl_4Cu_6N_{33.50}O_{16}S_2$	$C_{38}H_{50}Cl_2Cu_4N_{22}O_9S_2$	$C_{22}H_{31}ClCu_2N_{12}O_5S$	$C_{21}H_{27}ClCu_2N_{12}O_4S$
M_r	1034.81	829.61	664.77	2098.20	1348.18	738.18	706.14
T/K	163(2)	168(2)	168(2)	163(2)	168(2)	168(2)	168(2)
Space group	$P2_1/n$	$P2_1/c$	$C2/c$	$P\bar{1}$	$P\bar{1}$	$P2_1/c$	$P2_1/c$
Crystal System	Monoclinic	Monoclinic	Monoclinic	Triclinic	Triclinic	Monoclinic	Monoclinic
a/Å	12.025(5)	17.905(4)	28.144(16)	12.686(4)	12.203(3)	17.297(6)	16.854(6)
b/Å	11.018(5)	12.063(2)	12.482(8)	14.481(4)	15.172(4)	11.743(4)	11.891(4)
c/Å	21.943(5)	15.845(3)	16.676(10)	24.546(7)	15.802(4)	16.131(6)	16.280(5)
α/°	90	90	90	87.383(4)	102.925(4)	90	90
β/°	94.246(5)	92.812(3)	109.22(4)	84.732(4)	96.256(4)	112.506(5)	118.727(3)
γ/°	90	90	90	64.267(4)	112.461(4)	90	90
V/Å^3	2899.3(19)	3418.2(11)	5532(6)	4045(2)	2572.9(12)	3027.1(18)	2861.0(16)
Z	4	4	8	2	2	4	4
D_c	2.371	1.612	1.596	1.723	1.740	1.620	1.639
Crystal size/mm	0.60 × 0.14 × 0.11	0.25 × 0.24 × 0.14	2.00 × 1.00 × 0.01	0.51 × 0.31 × 0.04	0.8 × 0.5 × 0.4	0.34 × 0.17 × 0.13	0.45 × 0.26 × 0.04
μ/mm^{-1}	11.848	1.466	1.728	1.818	1.891	1.617	1.705
F(000)	1944	1696	2720	2134	1372	1512	1440
θ Range	2.00–26.70	2.04–27.51	1.80–23.46	1.91–27.61	2.04–26.43	2.15–26.43	2.20–26.38
Refls. collected	35598	26314	10769	51507	28660	38745	35477
Data/restr./param.	5996/0/393	7367/0/449	3047/0/357	16862/24/1251	10278/0/713	6163/0/394	5770/0/375
GOF	1.074	1.024	1.112	1.088	1.046	1.017	1.260
$R1$, $wR2$ ($F > 4\sigma(F)$)	0.0379, 0.0993	0.0389, 0.0948	0.0614, 0.1411	0.0686, 0.1672	0.0382, 0.1062	0.0496, 0.0845	0.0848, 0.1165
$R1$, $wR2$ (all data)	0.0491, 0.1044	0.0487, 0.0991	0.0850, 0.1561	0.1043, 0.1761	0.0449, 0.1099	0.0779, 0.0944	0.1315, 0.1267
$\Delta\rho_{max/min}$/e Å^{-3}	3.981/−1.940	0.672/−0.694	1.096/−0.746	1.163/−0.895	3.700/−1.231	0.540/−0.416	0.524/−0.603

{[Cu^{II}_2(L2)(NCS)](ClO$_4$)}$_x$ (6), crystals as 6·DMF. Crystals of {[Cu^{II}_2(L2)(NCS)][Cu^{II}_2(L2)(SCN)](ClO$_4$)$_2$}$_x$ (**5**) were redissolved in DMF and the clear blue–green solution diffused with diethyl ether to yield blue–green crystals of {[Cu^{II}_2(L2)(NCS)](ClO$_4$)}$_x$·DMF (44%). FAB *m*/*z* (rel. intensity): 154 (88), 307 (11), 506 (17), 607 (22). Found C, 35.72; H, 3.88; N, 22.69; S, 4.51. $C_{22}H_{31}N_{12}O_5SClCu_2$ requires C, 35.87; H, 4.24; N, 22.83; S, 4.34%. IR (KBr disk) (ν_{max}/cm^{-1}): 2130, 1617, 1485, 1411, 1089, 620. The crystals lost solvent very quickly.

{[Cu^{II}_2(L2)(NCS)](ClO$_4$)}$_x$ (6), crystals as 6·MeCN. Crystals of {[Cu^{II}_2(L2)(NCS)](ClO$_4$)}$_x$·DMF (**6**·DMF) were redissolved in MeCN and the clear blue–green solution diffused with diethyl ether to yield blue–green crystals of {[Cu^{II}_2(L2)(NCS)](ClO$_4$)}$_x$·MeCN (88%). FAB *m*/*z* (rel. intensity): 154 (89), 307 (11), 506 (17), 607 (24). Found C, 35.72; H, 3.88; N, 23.69; S, 4.51. $C_{22}H_{31}N_{12}O_5SClCu_2$ requires C, 35.79; H, 3.87; N, 23.87; S, 4.54%. IR (KBr disk) (ν_{max}/cm^{-1}): 2131, 1617, 1485, 1412, 1087, 620.

X-Ray crystallography

X-Ray data were collected on a Bruker SMART diffractometer (λ = 0.71073 Å) and the structures solved and refined (all non-hydrogen atoms anisotropic) using SHELXS and SHELXL.[31] Details of the crystal structures are collected in Table 8 and additional notes referring to particular structures are detailed below.

[Pb^{II}_2(L2)](ClO$_4$)$_2$·MeCN, (1)·MeCN. Highest peaks (*Q*1 = 3.98, *Q*2 = 3.62, *Q*3 = 3.60, *Q*4 = 3.45) are residuals due to absorption and are all within 1 Å of the lead atoms.

[Cu^{II}_2(L2)(NCS)$_2$]·MeCN, (3)·MeCN. Data is 75% complete to $2\theta = 47°$.

{[Cu^{II}_2(L2)]$_3$(NCS)$_2$}(ClO$_4$)$_4$·1.5 MeCN, (4)·1.5 MeCN. Atoms C(61), O(5D), O(12A) and O(14A) were restrained using ISOR to aid convergence (restrained goodness of fit = 1.089). Positional disorder in perchlorate counterions [central chlorine atoms Cl(10), Cl(30), Cl(40) and Cl(50)] and one macrocycle alkyl chain [C(58), C(59), C(60)] was successfully modelled.

[Cu^{II}_2(L2)(NCS)]$_x$·H_2O, (5)·H_2O. One water molecule disordered over two sites.

CCDC reference numbers 207829–207835.

See http://www.rsc.org/suppdata/dt/b3/b304658c/ for crystallographic data in CIF or other electronic format.

Acknowledgements

We thank the Marsden Fund for funding a postdoctoral research fellowship (U. B. and K. H.) and the New Zealand Foundation for Research, Science, and Technology for funding a postdoctoral fellowship (C. V. D.). We acknowledge Professor W. T. Robinson and C. Richardson (University of Canterbury) for the X-ray data collections, B. M. Clark (University of Canterbury) for the FAB mass spectra and Dr C. D. Brandt (University of Otago) for his help.

References

1 R. H. Wiley, *J. Macromol. Sci., Chem.*, 1987, **24**, 1183; F. Abraham, M. Lagrenee, S. Sueur, B. Mernari and C. Bremard, *J. Chem. Soc., Dalton Trans.*, 1991, 1443.
2 S. Brooker and R. J. Kelly, *J. Chem. Soc., Dalton Trans.*, 1996, 2117; S. Brooker, R. J. Kelly and G. M. Sheldrick, *J. Chem. Soc., Chem. Commun.*, 1994, 487.
3 S. Brooker, R. J. Kelly, B. Moubaraki and K. S. Murray, *Chem. Commun.*, 1996, 2579.
4 S. Brooker, R. J. Kelly and P. G. Plieger, *Chem. Commun.*, 1998, 1079; S. Brooker, P. G. Plieger, B. Moubaraki and K. S. Murray, *Angew. Chem., Int. Ed.*, 1999, **38**, 408; S. Brooker, S. J. Hay and P. G. Plieger, *Angew. Chem., Int. Ed.*, 2000, **39**, 1968; S. Brooker, D. J. de Geest, R. J. Kelly, P. G. Plieger, B. Moubaraki, K. S. Murray and G. B. Jameson, *J. Chem. Soc., Dalton Trans.*, 2002, 2080; S. Brooker, *Eur. J. Inorg. Chem.*, 2002, 2535.
5 S. Brooker, T. C. Davidson, S. J. Hay, R. J. Kelly, D. K. Kennepohl, P. G. Plieger, B. Moubaraki, K. S. Murray, E. Bill and E. Bothe, *Coord. Chem. Rev.*, 2001, **216–217**, 3.
6 J. G. Haasnoot, *Coord. Chem. Rev.*, 2000, **200–202**, 131.
7 U. Beckmann and S. Brooker, *Coord. Chem. Rev.*, 2003, in press.
8 M. H. Klingele and S. Brooker, *Coord. Chem. Rev.*, 2003, **241**, 119.
9 R. Prins, P. J. M. L. Birker, J. G. Haasnoot, G. C. Verschoor and J. Reedijk, *Inorg. Chem.*, 1985, **24**, 4128.
10 L. Antolini, A. C. Fabretti, D. Gatteschi, A. Giusti and R. Sessoli, *Inorg. Chem.*, 1990, **29**, 143; J. Krober, E. Codjovi, O. Kahn, F. Groliere and C. Jay, *J. Am. Chem. Soc.*, 1993, **115**, 9810; P. J. van Koningsbruggen, D. Gatteschi, R. A. G. de Graaff, J. G. Haasnoot, J. Reedijk and C. Zanchini, *Inorg. Chem.*, 1995, **34**, 5175; Y. Garcia, P. J. van Koningsbruggen, G. Bravic, P. Guionneau, D. Chasseau, G. L. Cascarano, J. Moscovici, K. Lambert, A. Michalowicz and O. Kahn, *Inorg. Chem.*, 1997, **36**, 6357; Y. Garcia, O. Kahn, L. Rabardel, B. Chansou, L. Salmon and J. P. Tuchagues, *Inorg. Chem.*, 1999, **38**, 4663; A. F. Stassen, M. de-Vos, P. J. van Koningsbruggen, F. Renz, J. Ensling, H. Kooijman, A. L. Spek, J. G. Haasnoot, P. Gütlich and J. Reedijk, *Eur. J. Inorg. Chem.*, 2000, 2231.
11 P. J. van Koningsbruggen, J. G. Haasnoot, H. Kooijman, J. Reedijk and A. L. Spek, *Inorg. Chem.*, 1997, **36**, 2487.
12 O. Kahn, *Chem. Br.*, 1999, **2**, 24.
13 W. R. Browne, C. M. O'Connor, H. P. Hughes, R. Hage, O. Walter, M. Doering, J. F. Gallagher and J. G. Vos, *J. Chem. Soc., Dalton Trans.*, 2002, 4048.
14 U. Beckmann, S. Brooker, C. V. Depree, J. D. Ewing, B. Moubaraki and K. S. Murray, *Dalton Trans.*, 2003, **7**, 1308.
15 J. de Mendoza, J. M. Ontoria, M. C. Ortega and T. Torres, *Synthesis*, 1992, 398; J. M. Alonso, M. R. Martin, J. de Mendoza and T. Torres, *Heterocycles*, 1987, **26**, 989.
16 J. A. Duro, J. M. Ontoria, A. Sastre, W. Schafer and T. Torres, *J. Chem. Soc., Dalton Trans.*, 1993, 2595; P. Souza, A. I. Matesanz, A. Arquero and V. Fernandez, *Z. Naturforsch., Teil B*, 1994, **49**, 665; B. Cabezón, M. Irurzun, T. Torres and P. Vazquez, *Tetrahedron Lett.*, 1998, **39**, 1067; M. Nicolau, B. Cabezón and T. Torres, *J. Org. Chem.*, 2001, **66**, 89; B. Cabezón, A. Sastre, T. Torres, W. Schafer, J. J. Borras-Almenar and E. Coronado, *J. Chem. Soc., Dalton Trans.*, 1995, 2305; M. S. Rodriguez-Morgade, B. Cabezón, S. Esperanza and T. Torres, *Chem. Eur. J.*, 2001, **7**, 2407.
17 E. Alcalde, M. Gisbert, C. Alvarez-Rua and S. Garcia-Granda, *Tetrahedron*, 1996, **52**, 15189; E. Alcalde, N. Mesquida, L. Perez-Garcia, S. Ramos, M. Alemany and M. L. Rodríguez, *Chem. Eur. J.*, 2002, **8**, 474; E. Alcalde, M. Alemany, L. Perez-Garcia and M. L. Rodríguez, *J. Chem. Soc., Chem. Commun.*, 1995, 1239.
18 S. Ferrer, P. J. van Koningsbruggen, J. G. Haasnoot, J. Reedijk, H. Kooijman, A. L. Spek, L. Lezama, A. F. Arif and J. S. Miller, *J. Chem. Soc., Dalton Trans.*, 1999, 4269.
19 P. M. Slangen, P. J. van Koningsbruggen, J. G. Haasnoot, J. Jansen, S. Gorter, J. Reedijk, H. Kooijman, W. J. J. Smeets and A. L. Spek, *Inorg. Chim. Acta*, 1993, **212**, 289.
20 P. J. van Koningsbruggen, J. G. Haasnoot, R. A. G. de Graaff, J. Reedijk and S. Slingerland, *Acta Crystallogr., Sect. C*, 1992, **48**, 1923; W. M. E. Koomen-van-Oudenniel, R. A. G. de Graaff, J. G. Haasnoot, R. Prins and J. Reedijk, *Inorg. Chem.*, 1989, **28**, 1128.
21 P. M. Slangen, P. J. van Koningsbruggen, K. F. Goubitz, J. G. Haasnoot and J. Reedijk, *Inorg. Chem.*, 1994, **33**, 1121.
22 U. Beckmann, J. D. Ewing and S. Brooker, *Chem. Commun,*, 2003, 1690; U. Beckmann, C. V. Depree, J. D. Ewing, M. H. Klingele and S. Brooker, unpublished results.
23 C. Harding, D. McDowell, J. Nelson, S. Raghunathan, C. Stevenson, M. G. B. Drew and P. C. Yates, *J. Chem. Soc., Dalton Trans.*, 1990, 2521.
24 S. Ferrer, J. G. Haasnoot, J. Reedijk, E. Muller, M. Biagini-Cingi, A. M. Manotti-Lanfredi, F. Ugozzoli and C. Foglia, *J. Chem. Soc., Dalton Trans.*, 1992, 3029.
25 K. Nakamoto, *Infrared and Raman Spectra of Inorganic and Coordination Compounds Part B*, John Wiley and Sons Inc., New York, 1997.
26 D. F. T. Tuan, J. W. Reed and R. Hoffmann, *J. Mol. Struct. (Theochem)*, 1991, **232**, 111.
27 M. A. S. Goher, Q.-C. Yang and T. C. W. Mak, *Polyhedron*, 2000, **19**, 615; O. Teichert and W. S. Sheldrick, *Z. Anorg. Allg. Chem.*, 1999,

625, 1860; A. J. Blake, N. R. Brooks, N. R. Champness, M. Crew, L. R. Hanton, P. Hubberstey, S. Parsons and M. Schroder, *J. Chem. Soc., Dalton Trans.*, 1999, 2813; P. C. Healy, C. Pakawatchai, R. I. Papasergio, V. A. Patrick and A. H. White, *Inorg. Chem.*, 1984, **23**, 3769; S. A. Barnett, A. J. Blake, N. R. Champness and C. Wilson, *CrystEngComm*, 2000, 5; O. Teichert and W. S. Sheldrick, *Z. Anorg. Allg. Chem.*, 2000, **626**, 2196; R. Hehl and G. Thiele, *Z. Anorg. Allg. Chem.*, 2000, **626**, 2167; M. A. S. Goher, R.-J. Wang and T. C. W. Mak, *J. Coord. Chem.*, 1996, **38**, 151; A. J. Blake, N. R. Champness, M. Crew, L. R. Hanton, S. Parsons and M. Schroder, *J. Chem. Soc., Dalton Trans.*, 1998, 1533; C. L. Raston, B. Walter and A. H. White, *Aust. J. Chem.*, 1979, **32**, 2757; T. Rottgers and W. S. Sheldrick, *Z. Anorg. Allg. Chem.*, 2001, **627**, 1976; O. A. Babich, V. N. Kokozay and V. A. Pavlenko, *Polyhedron*, 1996, **15**, 2727; H. Krautscheid, N. Emig, N. Klaassen and P. Seringer, *J. Chem. Soc., Dalton Trans.*, 1998, 3071; J. A. Rusanova, K. V. Domasevitch, O. Y. Vassilyeva, V. N. Kokozay, E. B. Rusanov, S. G. Nedelko, O. V. Chukova, B. Ahrens and P. R. Raithby, *J. Chem. Soc., Dalton Trans.*, 2000, 2175.

28 J. Lang, H. Kawaguchi, S. Ohnishi and K. Tatsumi, *Chem. Commun.*, 1997, 405.

29 L. A. Kovbasyuk, O. A. Babich and V. N. Kokozay, *Polyhedron*, 1997, **16**, 161.

30 J. A. Real, A. B. Gaspar, V. Niel and M. C. Muñoz, *Coord. Chem. Rev.*, 2003, **236**, 121.

31 G. M. Sheldrick, *Acta Crystallogr., Sect. A*, 1990, **46**, 467; G. M. Sheldrick, *Methods Enzymol.*, 1997, **276**, 628; G. M. Sheldrick and T. R. Schneider, *Methods Enzymol.*, 1997, **277**, 319.